

Modeling of a Back-Illuminated HgCdTe MWIR Avalanche Photodiode with Alloy Gradients

This content has been downloaded from IOPscience. Please scroll down to see the full text.

2015 J. Phys.: Conf. Ser. 647 012051

(<http://iopscience.iop.org/1742-6596/647/1/012051>)

View [the table of contents for this issue](#), or go to the [journal homepage](#) for more

Download details:

IP Address: 193.156.44.209

This content was downloaded on 18/02/2016 at 14:02

Please note that [terms and conditions apply](#).

Modeling of a Back-Illuminated HgCdTe MWIR Avalanche Photodiode with Alloy Gradients

A. K. Storebø and T. Brudevoll

Norwegian Defence Research Establishment, PO Box 25, 2007 Kjeller, Norway

E-mail: asta-katrine.storebo@ffi.no

Abstract. We present results from 2D Monte Carlo simulations of a mid-wave infrared (MWIR) back-illuminated planar n-on-p HgCdTe electron-initiated avalanche photodiode (e-APD). The main objective of this work has been to study the dependence of the multiplication gain, excess noise factor, and response time on the position where the incident photon is absorbed. We also quantify the effects of the naturally occurring vertical alloy gradient electric fields in APDs grown by liquid phase epitaxy. The simulated gain is relatively independent of the excitation position, but a small increase is observed near the edges of the APD. The excess noise factor is around 1.2 for all positions. It is found that the alloy gradient field helps to speed up the response of the device, especially for excitation positions far away from the multiplication region.

1. Introduction

HgCdTe (MCT) electron-initiated avalanche photodiodes (e-APDs) are characterized by high sensitivity and gain combined with low avalanche multiplication noise [1], [2]. These properties make them well suited for detection of very low radiation levels, such as in space imaging systems and laser-based detection systems. MCT APDs designed for the mid- and long-wavelength infrared regions, with cadmium alloy fractions less than 53%, operate mainly via single-carrier (electron) initiated multiplication. Therefore the gain becomes an exponential function of the reverse bias voltage. This simple gain mechanism results in an excess noise factor close to unity, largely independent of the gain. In addition, the response time can be very short, thus gain-bandwidth products in excess of 1 THz become possible. A great deal of modeling work on APDs have focused on obtaining phenomenological analytical relations describing the dependence of multiplication gain on reverse bias voltage or depletion layer geometry [3]. Other efforts have explored the various carrier interactions in more detail with Monte Carlo techniques [4]. In the present paper, we study the dependence of these properties on the position of the initial photo-excitation for a back-illuminated mid-wave infrared MCT APD, using 2D Monte Carlo simulation. We also study the effects of the naturally occurring vertical alloy gradient electric fields in the p-type absorption layer of APDs grown by liquid phase epitaxy [5], [6], [7].

2. APD structure

Details of the simulated APD are shown in figure 1. It is smaller, but geometrically similar to the planar structure discussed in [8], and larger than the other designs investigated in [4]. The large devices studied in [8] allowed the position-dependent multiplication gain to be probed experimentally



by focusing radiation onto different spots on the APD surface. Then a two-gain model consisting of a constant gain in the central region and an enhanced gain at the edges of the APD was introduced as a means of explaining the observations. It is therefore of interest to see if some of these effects could be confirmed by the Monte Carlo simulations in the present work.

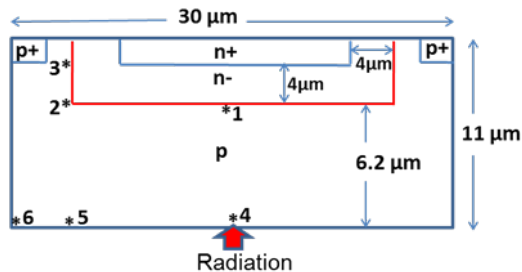


Figure 1. Layout of the planar electron-initiated APD. The doped-in carrier concentrations are $p = 2 \cdot 10^{16} \text{ cm}^{-3}$, $n^- = 5 \cdot 10^{14} \text{ cm}^{-3}$, and $p^+ = n^+ = 2 \cdot 10^{17} \text{ cm}^{-3}$ for the contacts. Numbers 1-6 indicate different initial photo-excitation positions used in the simulations.

It has been speculated whether the alloy gradient quasi-electric fields (AGFs) naturally arising in LPE-grown MCT materials may play a role in speeding up the transport of the initial photo-generated carriers, thus resulting in shorter response times [8]. Simulations were therefore carried out both with and without these AGFs. In simulations without alloy gradients, the Cd alloy fraction, x , was set to a constant value of 0.28. In simulations with alloy gradients, x was set to decrease exponentially from 0.33 at the entrance face (i.e. cut-off at 4 μm) to a value of 0.28 at the p-n junction, according to the expression $x = 0.27 + 0.06 \cdot \exp(-z/3.7)$, where z is the distance from the irradiated back surface in μm [5]. The effect of the gradient can be described by two bare AGFs, one affecting holes and the other affecting electrons. Free, doped-in electric charges then respond and move according to one of the two bare AGFs, resulting in a self-consistent equilibrium bias electric field affecting both carrier types. The alloy gradient and associated electron- and hole bare AGFs are shown in figure 2.

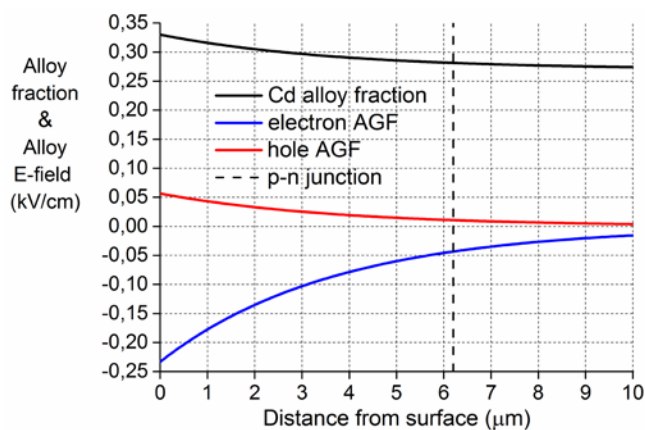


Figure 2. Cd alloy fraction and bare alloy gradient quasi-electric fields in undoped HgCdTe as a function of distance from the irradiated back surface at 77 K. The dashed line indicates the position of the p-n junction.

The importance of the alloy gradient field may depend on the thickness of the p-type absorption layer, since the gradients are located near the outer surface. A thick p-type absorption layer is important for the ability to operate near the cutoff wavelength of the MCT material. The p-layer is chosen to be 6.2 μm thick in the present work, and the AGF is fairly weak at the p-n junction.

3. Simulation model

In order to obtain a small photo-generated signal from a large background of free charge carriers, we performed a linearised, small signal analysis with single electron/hole resolution on top of a background bias electric field calculation. The bias calculation was carried out in the super-particle picture, and the resulting electric field was smoothed before it was used in the small signal analysis as a 'frozen field'. Each APD simulation consisted of 1000 different single-photon absorption events at the same position. Six excitation positions were considered, as indicated in figure 1. Impact ionization

was modeled with a simple Keldysh type expression, also used in other work [9], and terminal currents were calculated according to [10], [11].

Carrier transport in the p-type absorption layer can be affected by ambipolar effects varying with irradiation and doping, and at high reverse bias carrier tunneling through the p-n junction may create additional electron-hole pairs. Such processes were not included here, only ionized impurity and phonon scattering mechanisms were considered.

4. Results and discussion

All simulation results presented below are for 7 V reverse bias and 77 K temperature. Figure 3 shows four examples of simulated electron tracks with/without an AGF, for photo-excitation at two different positions (4 and 5) on the irradiated surface. It is evident that the AGF helps to bring the electrons on a more direct path towards the p-n junction.

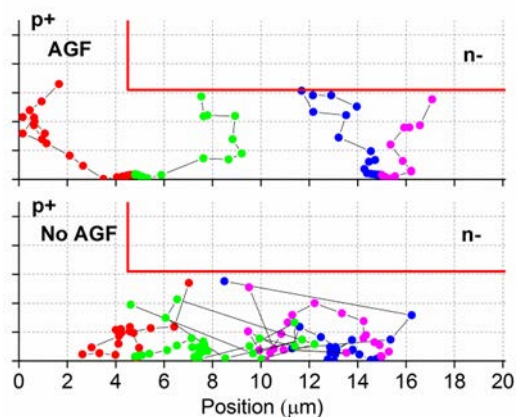


Figure 3. Four simulated electron tracks, showing particle positions at given time intervals, starting with initial photo-excitation at positions 4 and 5 respectively, with and without the presence of an AGF. The p-n junction is indicated in red.

The lower plot in figure 4 gives an example of the simulated times of arrival at the contacts for electrons and holes in a case where the APD gain $M = 81$. The upper plot shows the corresponding terminal current on the n-contact under the assumption of a constant terminal voltage. All electrons are collected within only 50 ps, whereas the holes take several ns to arrive at the contacts, i.e. it is the electrons that provide the fast response of the APD. Figure 5 shows a histogram of APD gain values (M) from 1000 simulations at position 1, with a mean value $M_{\text{mean}} = 54$, and a standard deviation of 23, resulting in a calculated excess noise factor $F \approx 1.2$ from the expression shown in figure 5.

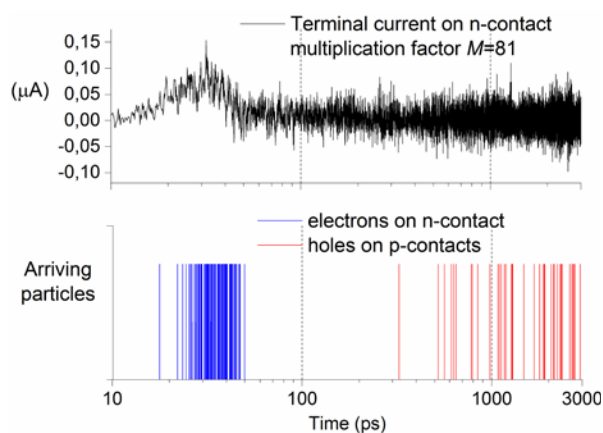


Figure 4. Terminal current plot and corresponding carrier time-of-arrival plot for an absorbed photon at position 1, with AGF and for $M = 81$.

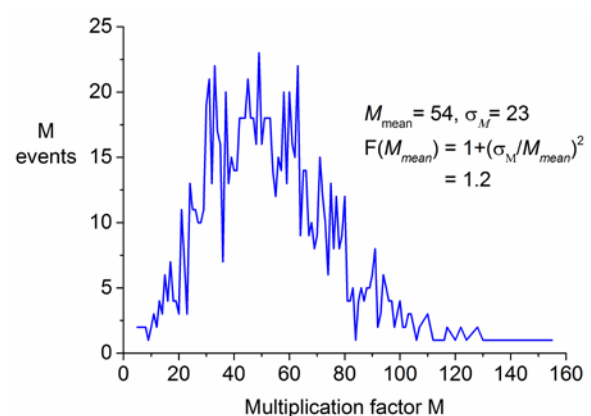


Figure 5. Histogram of electron multiplication events for photo-excitation at position 1.

Table 1. Simulation results for 7 V reverse bias at 77 K temperature. The response time, t_R (ns), has here been defined as the time when all excess electrons have reached their contact.

Position	M (AGF)	F (AGF)	t_R (AGF)	M (no AGF)	F (no AGF)	t_R (no AGF)
1	52	1.2	0.06	52	1.2	0.09
2	58	1.2	0.11	57	1.2	0.19
3	55	1.2	0.08	55	1.2	0.10
4	53	1.2	0.09	52	1.2	0.24
5	56	1.2	0.13	57	1.2	0.29
6	57	1.2	0.16	57	1.2	0.33

The main simulation results are summarized in Table 1. The APD gain is relatively independent of the excitation position, but a small increase is observed near the edges of the APD (positions 2, 3, 5, and 6), which has also been observed experimentally [8]. The excess noise factor is around 1.2 for all positions. It is evident that the electron AGF helps to speed up the response, not only for photons absorbed near the entrance face where the bare alloy field is strong (225 V/cm for electrons), but also for photons absorbed near the p-n junction where the alloy field is weak (50 V/cm for electrons). Response times are much shorter than electron lifetimes (typically 30 ns), so that virtually all photo-electrons will reach the multiplication region at the p-n junction.

5. Conclusions

We have seen that the dynamic response of a particular APD is indeed affected by alloy gradients. There were also notable positional differences in avalanche gain which apparently do not translate into positional variations in excess noise.

References

- [1] Beck J D, Wan C-F, Kinch M A, and Robinson J E 2001, *Proc. SPIE* **4454**, 188
- [2] Singh A, Srivastav V, Pal R 2011, *Optics & Laser Technology* **43**,1358
- [3] Rothman J, Mollard L, Bosson S, Vojetta G, Foubert K, Gatti S, Bonnouvrier G, Salveti F, Kerlain A, Pacaud O 2012, *J. Electron. Mater.* **41**, 2928
- [4] Bellotti E, Moresco M, and Bertazzi F 2011, *J. Electron. Mater.* **40**(8):1651-1656
- [5] LoVecchio P, Wong K, Parodos T, Tobin S P, Hutchins M A, and Norton P W 2004, *Proc. SPIE* **5564**, 65
- [6] Kraut E A, Vac J 1989, *Sci. Technol. A* **7** (2), 420
- [7] Nasrallah S A-B, Mnasri S, Sfina N, Bouarissa N, Said M 2011, *J. Alloys and Compounds* **509**, 7677
- [8] Reine M B, Marciniak J W, Wong K K, Parodos T, Mullarkey J D, Lamarre P A, Tobin S P, Minich R W, Gustavsen K A, Compton M, and Williams G M 2008, *J. Electron. Mater.* **37**, 1376
- [9] Derelle S, Bernhardt S, Haïdar R, Deschamps J, Primot M B, Rothman J, Rommeluere S, and Gue'rineau N 2009, *J. Electron. Mater.* **38**, 1628
- [10] Shockley W J 1938, *Appl. Phys.* Vol. **9**, 635
- [11] Ramo S 1939, *Proceedings of the IRE* Vol. **27**, 584